

## Origins of Complex Self-Assembly in Block Copolymers

M. W. Matsen\* and F. S. Bates

Department of Chemical Engineering and Materials Science,  
University of Minnesota, Minneapolis, Minnesota 55455

Received May 21, 1996

Revised Manuscript Received August 19, 1996

Amphiphilic molecules are renowned for their ability to partition chemically immiscible components into nanoscale domains. Often these domains exhibit intriguing complex periodic geometries with long-range order. Surprisingly, the diverse systems that self-assemble in this manner, surfactants, lipids, soaps, and block copolymers, exhibit topologically identical geometries, suggesting to researchers that a common set of principles govern amphiphilic phase selection. From this association has emerged the belief that constant mean curvature (CMC) interfaces are generally good models for block copolymer microdomain geometries. By taking advantage of new developments in polymer theory, we accurately examine this hypothesis for the first time, and find it to be wrong. Furthermore, our study reveals new explanations for complex phase selection that are relevant to numerous block copolymer systems.

A block copolymer consists of chemically distinct polymer chains (i.e., blocks) joined together to form a single macromolecule. As a consequence of a general tendency for the blocks to separate, tempered by the restriction imposed by the covalent bonds that connect them, these molecules exhibit amphiphilic behavior. Even in the simplest case, AB diblock copolymers, a rich assortment of ordered phases has been documented.<sup>1–8</sup> The composition of the AB diblock (i.e., the volume fraction  $f$  of block A) controls the geometry of the structure (see Figure 1). For nearly symmetric diblocks ( $f \sim 1/2$ ), a lamellar (L) phase occurs. For moderate asymmetries, a complex bicontinuous state, known as the gyroid (G) phase, has been observed in which the minority blocks form domains consisting of two interweaving threefold-coordinated lattices.<sup>1,2</sup> (Prior to the discovery of the G phase, a double-diamond (D) structure formed from two fourfold-coordinated lattices<sup>3</sup> was erroneously associated with the bicontinuous state in these materials.<sup>4</sup>) Another complex structure, the perforated lamellar (PL) phase, occurs when the minority-component layers of the L phase develop a hexagonal arrangement of passages.<sup>5</sup> At yet higher asymmetries, the minority component forms hexagonally packed cylinders (C) and then spheres (S) arranged on a body-centered cubic lattice. Eventually, as  $f \rightarrow 0$  or 1, a disordered phase results.

The complete mean field or rather self-consistent field theory (SCFT) for block copolymers was developed by Helfand and co-workers.<sup>9</sup> However, at the time of its development, it had to be supplemented with approximations limiting its effectiveness. Nevertheless, important advances were made by examining this theory in the limits of weak<sup>10</sup> and strong<sup>11</sup> segregation. (The degree to which the A and B blocks segregate is determined by the product  $\chi N$ , where  $\chi$  is the Flory–Huggins A/B interaction parameter and  $N$  is the total

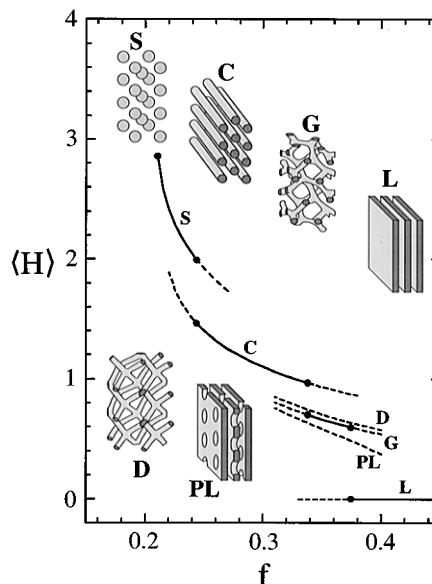


**Figure 1.** Area-averaged mean curvature  $\langle H \rangle$  as a function of the A-block volume fraction  $f$  for each of the structures shown schematically calculated using self-consistent mean-field theory.<sup>14,15</sup> The stable and metastable states are shown with solid and dashed lines, respectively, and transitions are denoted by dots. As the molecules become asymmetric, structures with more curvature are preferred.

degree of polymerization.) The combination of these works established that the underlying physics controlling block copolymer phase behavior involves a competition between interfacial tension and the entropic penalty for stretching polymer coils so as to fill space uniformly. The balance determines the equilibrium size of the microdomains and dictates the geometry of the structure. Although these earlier approaches correctly predicted the classical phases (i.e., L, C, and S),<sup>10,11</sup> they failed to account for the more recently discovered complex phases (i.e., G and PL).<sup>12,13</sup>

With new advances,<sup>14</sup> it is now possible to implement the full SCFT. The first calculations<sup>14,15</sup> to do so evaluated the free energies of the structures described above and established the phase diagram. This demonstrated that complex phase behavior occurs in the intermediate-segregation regime as opposed to the weak- and strong-segregation regimes treated by Leibler<sup>10</sup> and Semenov,<sup>11</sup> respectively. For intermediate segregation (e.g.,  $\chi N = 20$ ), the new calculations predict the sequence  $L \rightarrow G \rightarrow C \rightarrow S \rightarrow$  disordered as  $f$  progresses from  $1/2$  to either 0 or 1. Although PL is absent from this sequence, it is nearly stable at the L/G phase boundary, consistent with where it is observed experimentally.<sup>6</sup> This supports very recent experiments indicating that the PL structure is only a long-lived metastable state. The D phase is clearly unstable, in agreement with current experiments.<sup>4,6</sup> Given this theoretical accomplishment, we now probe deeper into the theory<sup>14</sup> to examine the physical factors responsible for complex phase behavior. As described below, the explanation lies in the detailed shape of the dividing interface between the A and B microdomains.

Earlier works, such as that of Semenov,<sup>11</sup> illustrate that the phase transitions are driven by a tendency to curve the interface as the diblocks become asymmetric in composition. The curvature allows the molecules to balance the degree of stretching between the A and B blocks. We demonstrate this quantitatively in Figure

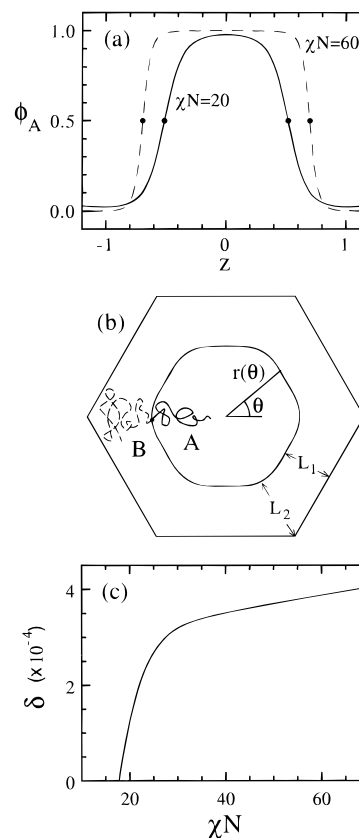
\* Present address: Polymer Science Centre, University of Reading, Whiteknights, Reading RG6 6AF, UK.

1 by evaluating the area-average ( $H$ ) of the mean curvature  $H \equiv 1/2(C_1 + C_2)$  for each structure, where  $C_1$  and  $C_2$  are the principal curvatures<sup>16</sup> at a given point on the surface. (Throughout this paper, lengths are expressed in terms of the statistical end-to-end length of an unperturbed diblock.) The trend in Figure 1 is obvious; as  $f$  deviates from  $1/2$ , transitions occur to structures possessing more interfacial curvature. However, based on variations in  $\langle H \rangle$  alone, we might expect the sequence  $L \rightarrow PL \rightarrow G \rightarrow D \rightarrow C \rightarrow S \rightarrow$  disordered, indicating that something in addition to curvature is responsible for complex phase selection.

While the average  $\langle H \rangle$  of the mean curvature controls the sequence of phases, we will demonstrate that the standard deviation  $\sigma_H$  of the mean curvature governs the phase selection. According to an idea proposed by Thomas et al.,<sup>8</sup> interfacial tension is a dominating factor in block copolymers, and therefore structures adopt area-minimizing surfaces of constant mean curvature (CMC),<sup>16</sup> which implies  $\sigma_H \approx 0$ . Here, we demonstrate that there is a second equally important factor, packing frustration, which has been identified earlier by Gruner and co-workers for lipid-membrane forming systems<sup>17,18</sup> and subsequently suggested as a mechanism in block copolymers.<sup>2,7</sup> For block copolymers, this mechanism translates into a tendency to form domains of uniform thickness so that none of the molecules are excessively stretched, which causes  $\sigma_H$  to deviate from zero. Although this effect has been observed in ABC triblock copolymers,<sup>19</sup> it is typically regarded to be of minor importance. Below we show that this is not true, and that in fact it plays an instrumental role in complex phase selection.

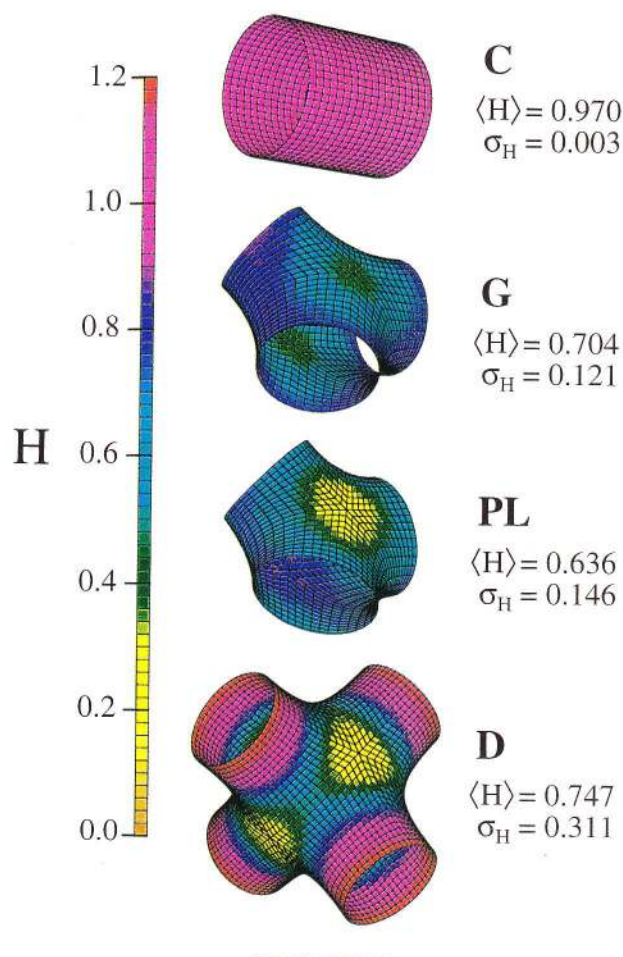
The above mechanisms are most easily discussed in terms of the C phase. Figure 2a shows the A-segment profile  $\phi_A$  through a cylinder for two degrees of segregation; this demonstrates both the increase in domain size and the decrease in interfacial width as  $\chi N$  increases. The interfacial surface, given by  $\phi_A = 1/2$  (see Figure 2a), is in general not circular.<sup>19</sup> It is well approximated by  $r(\theta) = r_0(1 + \delta \cos(6\theta))$ , where  $\delta$  measures the deviation from CMC. While the interfacial tension and packing considerations in the minority domain favor  $\delta = 0$ , the majority domain prefers  $\delta > 0$  so as to produce a more uniform thickness (i.e.,  $L_1 \approx L_2$  in Figure 2b). However, the frustration in the majority domain is small and  $\delta$  only deviates slightly from zero (see Figure 2c). In general, all the classical phases, L, C, and S, allow the molecules to pack efficiently and therefore do not exhibit significant variations from CMC. Contrary to published speculations,<sup>8</sup> the surface becomes less CMC-like at strong segregations as demonstrated by Figure 2c. The explanation is simple; as  $\chi N$  increases, the molecules become highly stretched relative to their unperturbed end-to-end statistical length, making it more difficult to fill the corners of the Wigner-Seitz cell. This observation that increasing  $\chi N$  amplifies the packing frustration will explain the absence of complex phases in the strong-segregation regime.

Unlike the classical phases, the complex phases suffer from high degrees of packing frustration, producing large deviations from CMC. Figure 3 shows the interfacial curvature over elementary units of the C, G, PL, and D structures calculated at the C/G transition in Figure 1. From the distribution of  $H$ , shown with the color scale, the average  $\langle H \rangle$  and standard deviation  $\sigma_H$  are calculated for each structure. While the C structure is nearly CMC (i.e.,  $\sigma_H \approx 0$ ), the complex phases all



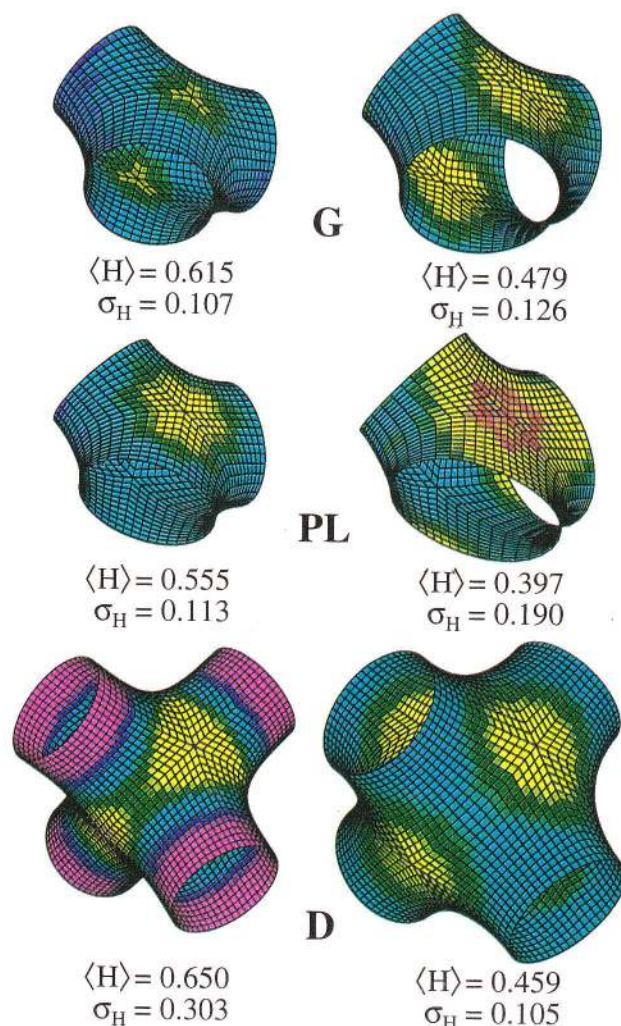
**Figure 2.** (a) A-segment profile across a minority domain of the cylinder (C) phase for  $f = 0.3378$  at two degrees of segregation,  $\chi N$ . The location of the interface defined by  $\phi_A = 1/2$  is indicated with dots. (b) The Wigner-Seitz hexagonal unit cell showing the interface between the A and B domains, and a representative diblock copolymer molecule. The interfacial shape is, in general, well described by  $r(\theta) = r_0(1 + \delta \cos(6\theta))$ . The stretching energy of the B domain prefers  $\delta \approx 0.03$  as illustrated in the figure so as to produce a relatively uniform thickness (i.e.,  $L_1 \approx L_2$ ). On the other hand, interfacial energy favors  $\delta = 0$  (i.e., a CMC surface). (c) The values of  $\delta$  that minimize interfacial tension and packing frustration for various segregations at  $f = 0.3378$ . The small values reflect a near absence of packing frustration in the C phase.

exhibit significant variations in  $H$ . The quantity  $\sigma_H$  directly reflects the inability of a structure to simultaneously minimize surface area and packing frustration, and therefore is correlated to its stability. We attribute a large portion of  $\sigma_H$  to frustration in the minority blocks, which have to fill the space at the center of the connectors in Figure 3. Naturally, this frustration is largest for the four-connector (i.e., the D phase). We believe G is favored over PL because its majority domain is less frustrated. Support for these deductions comes from calculations on diblock/homopolymer blends.<sup>20</sup> Adding homopolymer to the minority domain relieves packing frustration and can cause a transition from G to D. Similarly, adding homopolymer to the majority domain of G can stabilize PL. In Figure 4, we demonstrate that this increase in stability is accompanied by a decrease in  $\sigma_H$ ; further explanations for the trends in Figure 4 will be provided in a future publication. We note that this reduction in packing frustration closely resembles what is encountered with membrane-forming lipids and surfactant solutions.<sup>17</sup> Finally, the theoretical<sup>13,15,21</sup> and experimental<sup>7</sup> evidence that complex phases are unstable at strong segregations is rationalized by recalling that increasing  $\chi N$  exacerbates the packing frustration.



**Figure 3.** Interfacial surfaces associated with elementary units of the C, G, PL, and D structures calculated at the C/G phase boundary ( $\chi N = 20$  and  $f = 0.3378$ ). For each structure, the distribution of mean curvature  $H$  over the surface is indicated using the color scale, and the area-average  $\langle H \rangle$  and standard deviation  $\sigma_H$  of  $H$  is provided. The large values of  $\sigma_H$  reflect large degrees of packing frustration perturbing the interface away from CMC. Note that the three-connector of the G structure is planar, but the connector of the PL phase is slightly nonplanar, which produces an asymmetry between the top and bottom sides. The bar at the bottom represents one unit of length.

While the individual mechanisms that control complex phase selection are conceptually familiar,<sup>8,17,18</sup> to the best of our knowledge, there are no prior first-principles calculations thoroughly examining their relative importance. As a result, packing frustration has failed to receive proper recognition for its influence on block copolymer phase behavior. The full SCFT permits this study because it allows each microstructure to adjust its interface so as to minimize the energy associated with the combination of interfacial area and packing frustration. Other calculations<sup>13,21,22</sup> typically require *a priori* assumptions regarding interfacial shape, while those that do allow the segment profiles to adjust<sup>10,12</sup> are unable to treat experimentally relevant degrees of segregation where the interface is sufficiently developed to apply these concepts. Based on our SCFT calculation, packing frustration prevents the stability of the D and PL phases, and in general the stability of all complex phases in the strong-segregation limit. We have also illustrated which domains of the D and PL phases are most frustrated and how this can be relieved with the addition of an appropriate homopolymer. Such ideas will guide future efforts to stabilize new complex



**Figure 4.** Plots similar to Figure 3 using the same color scale, but calculated with added homopolymer. (The degree of polymerization of the homopolymer equals that of the diblock.) Surface units on the left each contain about 20% B homopolymer while those on the right have about 10% A homopolymer, which segregates to the majority and minority domains, respectively. In each case, structures are compared in the C + G two-phase coexistence region at  $\chi N = 20$ .

phases in block copolymer blends, and may shed additional light on the role of molecular frustration in ordered soft materials in general.

**Acknowledgment.** We thank G. H. Fredrickson, S. M. Gruner, D. A. Hajduk, and M. A. Hillmyer for critical readings of the manuscript. This work was supported by the Minnesota Supercomputer Institute and by the NSF (Grant DMR 94-05101).

#### References and Notes

- Schulz, M. F.; Bates, F. S.; Almdal, K.; Mortensen, K. *Phys. Rev. Lett.* **1994**, *73*, 86.
- Hajduk, D. A.; Harper, P. E.; Gruner, S. M.; Honeker, C. C.; Kim, G.; Thomas, E. L.; Fetters, L. J. *Macromolecules* **1994**, *27*, 4063.
- Thomas, E. L.; Alward, D. B.; Kinning, D. J.; Martin, D. C.; Handlin, D. L.; Fetters, L. J. *Macromolecules* **1986**, *19*, 2197.
- Hajduk, D. A.; Harper, P. E.; Gruner, S. M.; Honeker, C. C.; Thomas, E. L.; Fetters, L. J. *Macromolecules* **1995**, *28*, 2570.
- Hamley, I. W.; Koppi, K. A.; Rosedale, J. H.; Bates, F. S.; Almdal, K.; Mortensen, K. *Macromolecules* **1993**, *26*, 5959.
- Bates, F. S.; Schulz, M. F.; Khandpur, A. K.; Förster, S.; Rosedale, J. H.; Almdal, K.; Mortensen, K. *Faraday Discuss.* **1994**, *98*, 7.

- (7) Hajduk, D. A.; Gruner, S. M.; Rangarajan, P.; Register, R. A.; Fetters, L. J.; Honekar, C.; Albalak, R. J.; Thomas, E. L. *Macromolecules* **1994**, *27*, 490.
- (8) Thomas, E. L.; Anderson, D. M.; Henkee, C. S.; Hoffman, D. *Nature* **1988**, *334*, 598.
- (9) Helfand, E. *J. Chem. Phys.* **1975**, *62*, 999.
- (10) Leibler, L. *Macromolecules* **1980**, *13*, 1602.
- (11) Semenov, A. N. *Sov. Phys. JETP* **1985**, *61*, 733.
- (12) Hamley, I. W.; Bates, F. S. *J. Chem. Phys.* **1994**, *100*, 6813.
- (13) Fredrickson, G. H. *Macromolecules* **1991**, *24*, 3456. Olmsted, P. D.; Milner, S. T. *Phys. Rev. Lett.* **1995**, *74*, 829.
- (14) Matsen, M. W.; Schick, M. *Phys. Rev. Lett.* **1994**, *72*, 2660.
- (15) Matsen, M. W.; Bates, F. S. *Macromolecules* **1996**, *29*, 1091.
- (16) Anderson, D. M.; Davis, H. T.; Scriven, L. E.; Nitsche, J. C. *C. Adv. Chem. Phys.* **1990**, *77*, 337.
- (17) Gruner, S. M. *J. Phys. Chem.* **1989**, *93*, 7562.
- (18) Anderson, D. M.; Gruner, S. M.; Leibler, S. *Proc. Natl. Acad. Sci. U.S.A.* **1988**, *85*, 5364. Turner, D. C.; Gruner, S. M.; Huang, J. S. *Biochemistry* **1992**, *31*, 1356.
- (19) Gido, S. P.; Schwark, D. W.; Thomas, E. L.; Conçalves, M. *Macromolecules* **1993**, *26*, 2636.
- (20) Matsen, M. W. *Phys. Rev. Lett.* **1995**, *74*, 4225; *Macromolecules* **1995**, *28*, 5765.
- (21) Likhtman, A. E.; Semenov, A. N. *Macromolecules* **1994**, *27*, 3103.
- (22) Anderson, D. M.; Thomas, E. L. *Macromolecules* **1988**, *21*, 3221. Olmsted, P. D.; Milner, S. T. *Phys. Rev. Lett.* **1994**, *72*, 936.

MA960744Q